IEEE Photonics Journal
An IEEE Photonics Society Publication

Open Access

Temperature-Dependent Carrier Recombination and Efficiency Droop of AlGaN Deep Ultraviolet Light-Emitting Diodes

Volume 12, Number 1, February 2020

Zhangbao Peng
Weijie Guo
Tingzhu Wu
Ziquan Guo
Yijun Lu
Yicheng Zheng
Yue Lin
Zhong Chen

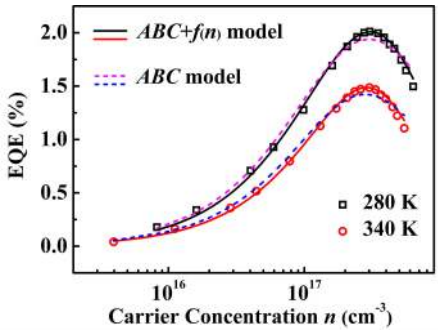

DOI: 10.1109/JPHOT.2019.2958311

Temperature-Dependent Carrier Recombination and Efficiency Droop of AlGaN Deep Ultraviolet Light-Emitting Diodes

Zhangbao Peng, Weijie Guo, Tingzhu Wu, Ziquan Guo, Yijun Lu, Yicheng Zheng, Yue Lin, and Zhong Chen

Department of Electronic Science, Fujian Engineering Research Center for Solid State Lighting, Collaborative Innovation Center for Optoelectronic Semiconductors and Efficient Devices, Xiamen University, Xiamen 361005, China

DOI:10.1109/JPHOT.2019.2958311

Manuscript received November 24, 2019; accepted December 4, 2019. Date of publication December 9, 2019; date of current version January 7, 2020. This work was supported in part by the National Natural Science Foundation of China under Grants 11604285, 51605404, 11504182, and 11674054; in part by the Science and Technology Project of Fujian Province under Grant 2018H6022; in part by the Natural Science Foundation of Fujian Province under Grant 2018J01103; in part by the Technological Innovation Project of Economic and Information Commission of Fujian Province; and in part by the Strait Postdoctoral Foundation of Fujian Province. *(Zhangbao Peng and Weijie Guo contributed equally to this work.)* Corresponding authors: Yue Lin; Zhong Chen (e-mail: yue.lin@xmu.edu.cn; chenz@xmu.edu.cn).

Abstract: We investigate temperature-dependent carrier transfer and efficiency droop on AlGaN-based deep ultraviolet light-emitting diodes. The Shockley-Read-Hall (SRH) recombination and carrier leakage are highly associated with the poor thermal stability. The existence of Auger recombination and carrier leakage is identified by the m-power method. A modified *ABC* model with an additional term $f(n)$ related to carrier leakage is employed to analyze the evolution of multiple recombination mechanisms. The SRH process strongly suppresses both Auger recombination and carrier leakage at low currents. At high currents, the latter two processes are responsible for the efficiency droop and exhibit an anti-correlation upon temperature.

Index Terms: Deep ultraviolet light-emitting diodes, recombination mechanisms, efficiency droop, *ABC* model.

1. Introduction

Deep ultraviolet light-emitting diodes (DUV LEDs), with emission wavelengths below 300 nm, are commonly manufactured with AlGaN-based multiple quantum wells (MQWs) [1]–[4]. High-photon-energy emissions are propitious in various fields, such as water sterilization, biological agent detection, covert communications, and solid state lighting [1], [5]–[7]. LEDs generally suffer from current-droop (*J*-droop) and temperature-droop (*T*-droop) [8], [9]. The former one refers to the reduction in external quantum efficiency (EQE) with increasing operating current, whereas the latter one refers to the reduction of EQE with increasing operating temperature [8], [9]. The *T*-droop originates from the high junction temperature, which affect the radiative and non-radiative recombination processes in the active region and possibly result in the thermal escape of carriers. Quantum barriers and electron-blocking layer (EBL) efficiently confine carriers into the active

region, but a portion of energetic carriers can still leak from MQWs, in the forms of thermionic overflow and/or defect-related tunneling courses, into p-doped layers where they conduct non-radiative recombination with holes, due to the polarization mismatch between MQWs and EBL, and high-defect structures [10], [11]. The mechanisms involved in efficiency droop in AlGaN-based DUV LEDs at high currents and/or high temperatures are still not clear. Experimental results have revealed that multiple sources, e.g., extend dislocations, quantum confined Stark effect (QCSE), carrier delocalization, Auger recombination, and carrier leakage, lead to the lower EQE and severer efficiency droop in AlGaN-based DUV LEDs than those in InGaN-based visible LEDs [10], [12]–[14]. In AlGaN-based DUV LEDs, the aluminum-rich EBL tends to prevent holes from entering MQWs, leading to a poor hole-injection efficiency [12], whereas the high-energy carriers are inclined to drift out of high-defect-density MQWs due to the insufficient restriction [15]. Although having been frequently used to comprehensively investigate the mentioned issues, the *ABC* model takes only into account the recombination inside MQWs [16], namely Shockley-Read-Hall (SRH) non-radiative recombination, radiative recombination, and Auger recombination. The carrier leakage, which occurs outside MQWs, is neglected in the conventional *ABC* model. Thus, a modified $ABC + f(n)$ model, where $f(n)$ is associated with the carrier leakage, proves a better precision than the conventional one when fits to the experimental data [17]. Due to the widely reported leakage in AlGaN-based DUV LEDs [15], [18], it is reasonable to introduce the leakage term $f(n)$ for a more detailed evaluation on the effect of carrier transfer and recombination.

In this work, we investigate the temperature dependence of carrier recombination mechanisms of the AlGaN-based DUV LEDs. We attribute the decrease in the thermal stability to the SRH recombination and carrier leakage. An *m*-power method is employed to distinguish recombination mechanisms at different injection currents. Furthermore, we utilize a modified $ABC + f(n)$ model to extract coefficients of the SRH recombination, radiative recombination, Auger recombination, and carrier leakage. Both current- and temperature-dependent contributions of different recombination mechanisms are quantitatively analyzed. At low current levels, SRH recombination contributes to the efficiency droop, whereas Auger recombination and carrier leakage exhibit an anti-correlation at high current levels and together dominate the efficiency droop.

2. Experimental Details

The sapphire substrate lies in sequence the 2-μm AlN buffer layer, 1-μm undoped $Al_{0.5}Ga_{0.5}N$, 2-μm Si-doped n-$Al_{0.6}Ga_{0.4}N$, six-period quantum structure of 3-nm $Al_{0.52}Ga_{0.48}N$ well and 10-nm $Al_{0.65}Ga_{0.35}N$ barriers, EBL of a 10-nm Mg-doped p-$Al_{0.75}Ga_{0.25}N$ layer, 50-nm p-doped $Al_{0.6}Ga_{0.4}N$ clad layer, and 100-nm Mg-doped p-GaN hole injection layer. The nominal peak emission wavelength peaks at $\sim$278 nm measured at 10 mA. The chip, 1 mm $\times$ 1 mm in size, is flip-chip bonded onto the surface mounted device (SMD) type AlN lead frame, which is covered by a quartz glass that serves as optical lens and protector. Finally, SMD packaged samples are soldered onto hexagonal aluminum metal core printed circuit board.

During the measurement, the heat-sink temperature mounting the samples is controlled between 280 K and 340 K with the increment of 10 K by using a TEC temperature controller (LED-850, Instrument Systems Corp., Germany). The EL data is collected in a 500-mm integrating sphere, which is connected to a spectrometer (Spectro-320e, Instrument Systems, Corp., Germany). An electric source meter (Keithley 2400, Keitheley Inc., USA) is used to drive samples at a series of currents, which range from 0.5 to 350 mA. To minimize the effect of self-heating on chips, we set the stop interval as 5 minutes before each measurement.

3. Results and Discussion

As temperature increases, the EQE decrease monotonically at the same forward current. However, for the same temperature, the EQE first increases then decreases as the current increases. The dependence of EQE on temperature and forward current is depicted in Fig. 1(a), which reveals a fact that both the *T*-droop and *J*-droop present a severe extent at the high current injection. We therefore

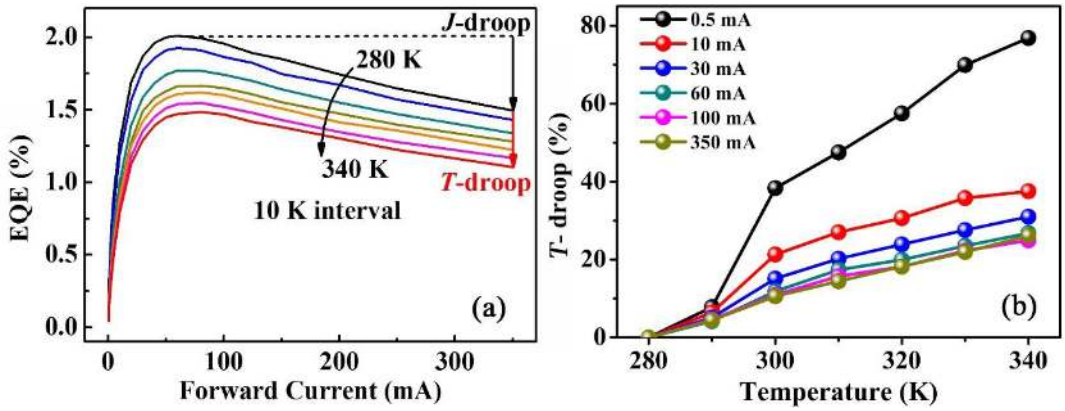

Fig. 1. (a) EQE as a function of forward current at different temperatures, (b) *T*-droop as a function of temperature at different forward currents.

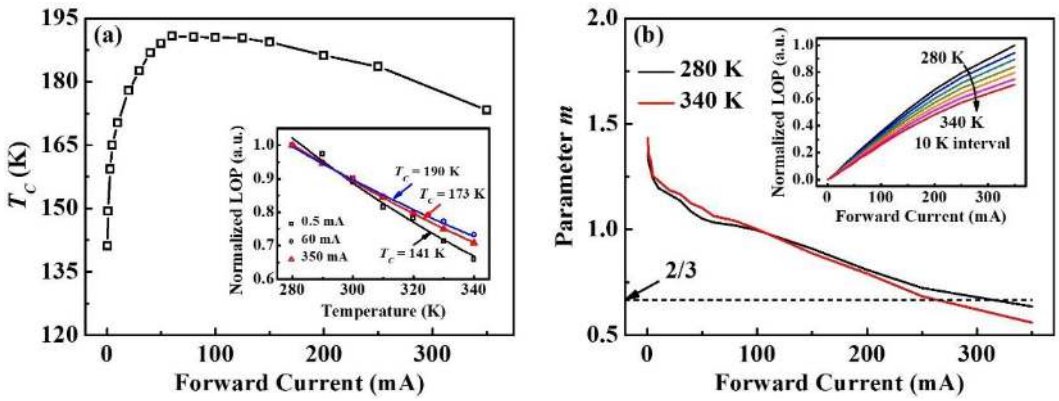

Fig. 2. (a) T_c as a function of forward current. Inset: Normalized LOP versus temperature and theoretical fitting result at 0.5 mA, 60 mA, and 350 mA, respectively. (b) Plots of parameter *m* at 280 K and 340 K. Inset: LOP as function of forward current at different temperatures.

deduce that the decrease in EQE is related to the concentration-rich and high-thermal-energy carriers, which probably exacerbate the Auger recombination and the carrier leakage, because of the thermal emission, large band offset caused by AlGaN barriers, and numerous defects in active layers [19]. The *T*-droops respect to 280 K as a function of temperature are also showed in Fig. 1(b). *T*-droop increases as the temperature increases from 280 K to 340 K. As the current increases from 0.5 mA to 60 mA, corresponding to the maximum EQE in Fig. 1(a), *T*-droop increases. The high *T*-droop at low currents originates from SRH recombination, and the reduction of *T*-droop is due to the radiative recombination gradually becomes dominant with increasing current [8]. Furthermore, with increasing the current increases from 100 mA to 350 mA, Auger recombination and carrier leakage become dominant and cause that the *T*-droop increases slightly.

Figure 2(a) depicts the current-dependent characteristic temperature (T_c), which is derived from the temperature dependence of the emission intensity [20]

$$L(T) = L(0)\exp\left(-\frac{T}{T_C}\right). \tag{1}$$

In Eq. (1), the $L(T)$ and $L(0)$ are the light output powers (LOPs) at operating temperature (T) and the absolute temperature (0 K), respectively. Three fitting data are plotted in the inset of Fig. 2(a). The T_c is an indicator of thermal stability of temperature-tolerant devices, i.e., the small value of

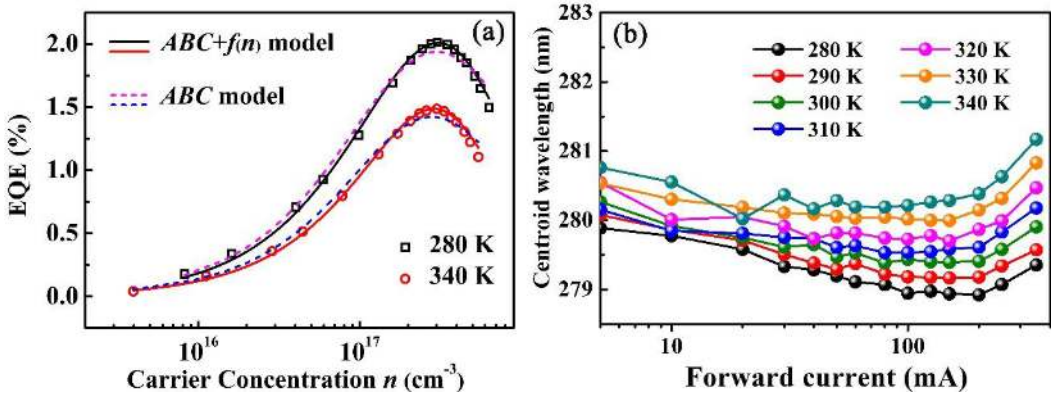

Fig. 3. (a) EQE versus carrier concentration and theoretical fitting at 280 K and 340 K, the solid curves fitted by $ABC + f(n)$ model and the dashed curves fitted by ABC model, (b) centroid wavelength of emission spectra of AlGaN-based DUV LEDs at different temperature.

T_c signifies the strong temperature dependence, whereas the large value of it means the weak temperature dependence. Compared with the changing of EQE upon a series of injection currents [Fig. 1], we find that a highly positive correlation exists between T_c and EQE. T_c is related to the activation energy of non-radiative recombination centers and the energy required to overcome the confining potentials [21], therefore, the larger T_c could suppress the non-radiative recombination and cause the relatively higher EQE.

Besides, temperature-dependent recombination mechanisms at different currents are extrapolated by the m-power method [22] $L = P \times I^m$, where P denotes a constant, and I is the forward current. The parameter m, derived from $\partial \ln L / \partial \ln I$, can qualitatively reflect the various recombination mechanisms of the DUV LED. The value of m approaches to 2 when SRH non-radiative recombination becomes dominant, and reaches 1 at the current corresponding to the peak of EQE, whereas varies from 1 to 2/3 when Auger recombination acts as the primary recombination mechanism [23]. As shown in Fig. 2(b), m decreases from 1.36 to 0.64 at 280 K and from 1.43 to 0.56 at 340 K, respectively. The relative rapid decline of m with increasing current at 340 K generates a cross point between curves of m as function of current for 280 K and 340 K. Meanwhile, curves of LOP as a function of current at different temperatures are plotted in the inset of Fig. 2(b).

On the basis of the above description, we propose an interpretation that intends to elaborate the relationship among EQE, T_c and m. At low injection currents, both low T_c and EQE can be attributed to the intensified SRH non-radiative recombination provided by the temperature sensibility of defect-related centers, which perform high m. However, at the current where EQE reaches its maximum (~60 mA), SRH centers are saturated and thus the radiative recombination rate achieves the peak, as a result of the elevated carrier interaction with radiative centers. When the m drops to 1, T_c also approaches its peak. At higher injection currents where EQE droop occurs, the non-radiative recombination increases, due to high-current-density processes other than SRH recombination. The decrease of T_c indicates that non-radiative processes induced by the high-injection should be as temperature sensitive as SRH recombination is. We can reasonably deduce that Auger recombination, as one type of temperature-dependent and non-radiative recombination mechanism, gradually evolves into the dominant factor with the increasing current, accompanied with the decreasing value of m below 1. Furthermore, considering that values of m below 2/3, we conjecture that the carrier leakage out of the active region, a multi-carrier loss mechanism, is brought into play as the current beyond 250 mA. The leakage may behaves a collection of various forms of non-radiative procedure, including thermionic emission of carriers out of MQWs, overflowing carriers not being captured by MQWs, and defect-assisted carrier tunneling [19].

As shown in Fig. 3(b), the centroid wavelength of emission spectra increase with temperature due to bandgap shrinking. As the forward current increases, the centroid wavelength exhibits blue-shift

in low current region, originating from the coulomb screening of the quantum-confined Stark effect (QCSE) in multiple quantum well [24], whereas the centroid wavelength become red-shift as the current beyond 200 mA due to the self-heating generated by the carrier leakage.

The *ABC* model is frequently employed to quantitatively investigate the effects of carrier recombination mechanisms, although it does not take the carrier leakage into account. However, the above analysis states that the carrier leakage process exerts a significant influence on the EQE droop, especially at high forward current. Therefore, we employ a modified *ABC* model with an additive term $f(n)$, which denotes the carrier leakage term in a power series with orders higher than 3 to further investigate the carrier transfer in the active layer. The total recombination rate can be described as $R = An + Bn^2 + Cn^3 + f(n)$, where A, B, and C denote coefficients of SRH non-radiative recombination, radiative recombination, and Auger recombination, respectively. According to the simplified method proposed by Schubert [25], we expand $f(n)$ in the form of Taylor series and only remain the fourth-order term Dn^4. Similar methodology has been conducted by Hahn's group [26], and they obtained an excellent fitting result on the integrated intensity data when the $f(n)$ term was considered as $Dn^{3.95}$, which also implies the primary process of carrier leakage. Since the EQE is directly proportional to the internal quantum efficiency (IQE), namely $\mathrm{EQE} = \eta_{\mathrm{inj}}\eta_{\mathrm{ext}}\mathrm{IQE}$, where η_{inj} and η_{ext} are the current injection efficiency and the light extraction efficiency, respectively, the carrier concentration (n) can be obtained by the equation [27]

$$n = \sqrt{\frac{\mathrm{EQE} \times I}{\eta_{\mathrm{inj}}\eta_{\mathrm{ext}}BqV_{\mathrm{QW}}}}, \tag{2}$$

where q and V_{QW} are the elementary charge and the volume of active region, respectively. Based on previous reports [28]–[30], η_{inj}, η_{ext} and B can be assumed to be ∼50%, ∼10%, and 2.1×10^{-11} $\mathrm{cm^3s^{-1}}$, respectively. The V_{QW} is calculated to be 7.8×10^{-8} $\mathrm{cm^3}$. The curves of EQE versus n are fitted at 280 K and 340 K as instances by the $ABC + f(n)$ model and *ABC* model, respectively. As shown in Fig. 3(a), comparison of the fitted curves of the two theoretical models with experimental data shows that there are larger deviation between the fitted curves of *ABC* model and the experimental data, particularly at high forward current, and that the inclusion of the $f(n)$ term is necessary.

As the temperature rises from 280 K to 340 K, values of A fitted by $ABC + f(n)$ model increase from 2.60×10^6 to 3.97×10^6 $\mathrm{s^{-1}}$, indicating that the monomolecular SRH non-radiative recombination is enhanced with the increasing temperature. Whereas, for *ABC* model, the fitted values of A increase from 2.38×10^6 to 3.52×10^6 $\mathrm{s^{-1}}$. Furthermore, for $ABC + f(n)$ model, the coefficients C of three-particle Auger recombination increase slightly from 1.41×10^{-29} to 2.04×10^{-29} $\mathrm{cm^6s^{-1}}$ as the temperature rises from 280 K to 340 K, which root in the interband Auger processes, and increase from 2.67×10^{-29} to 4.49×10^{-29} $\mathrm{cm^6s^{-1}}$ for *ABC* model. Therefore, without the $f(n)$ term, the fitted values of A are underestimated and C are overestimated. The fitted values of D increase monotonically from 2.21×10^{-47} to 4.75×10^{-47} $\mathrm{cm^9s^{-1}}$, which are approximately two orders of magnitude larger than the result published in a previous work [25], suggesting that drift-induced carrier leakage actually causes a grievous reduction in EQEs.

According to the numerical values of A, B, C, and D, we further calculate recombination rates of four types of mechanisms, namely An, Bn^2, Cn^3, and Dn^4, respectively. At 280 K [Fig. 4(a)] and 340 K [Fig. 4(b)], the SRH recombination term (An) rapidly enhances by two orders of magnitude from 10^{22} to 10^{24} $\mathrm{cm^{-3}s^{-1}}$ at the current range of 0.5 ∼ 60 mA, resulting a high fraction of 69∼81% out of the total recombination at low current of 10 mA [Fig. 4(c)]. However, the An term remains a weak increase afterwards (60∼350 mA), due to the saturation of non-radiative recombination centers at high injection currents. In view of both small values of T_c and EQE, and high values of m (> 1) at low current levels [Figs.1 and 2], we further identify that the temperature-sensitive and defect-related SRH recombination is associated with the poor thermal stability. In Fig. 4(d), the fraction of the SRH recombination measured at the current of 350 mA is largely mitigated, as the An acutely decreases to 12∼17% with increasing temperature. The proportion of Bn^2, representing the

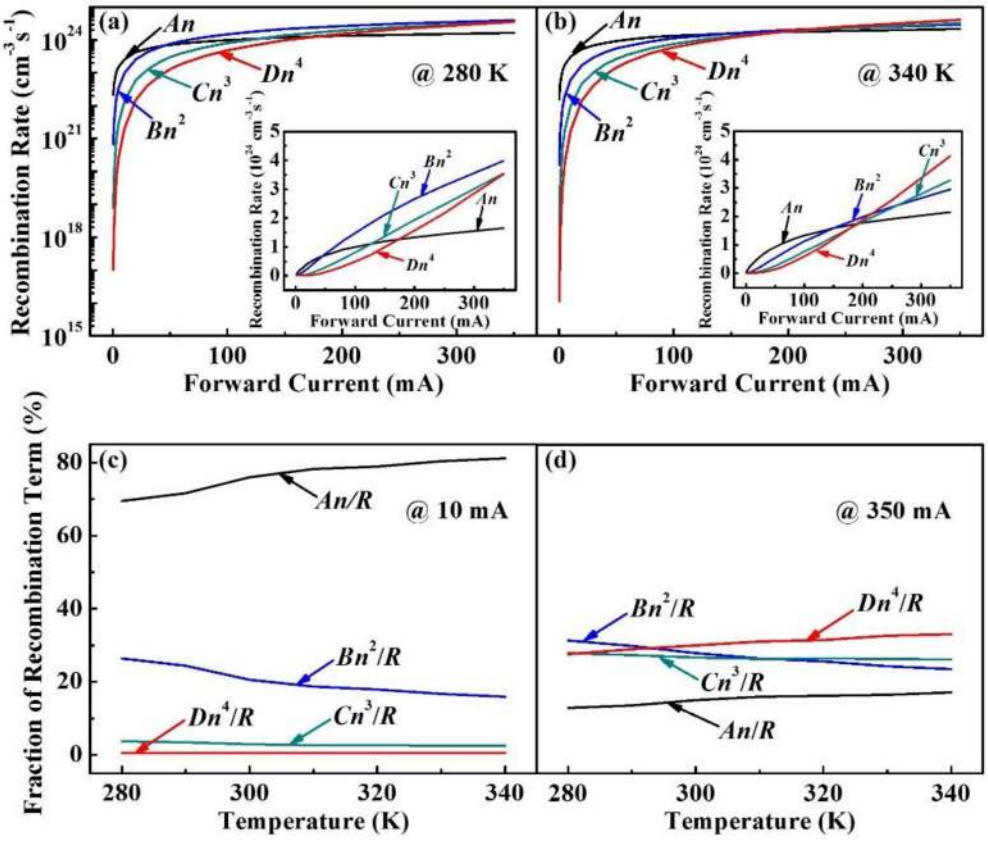

Fig. 4. Semi-log type of extracted recombination rates with respect to coefficients *A*, *B*, *C*, and *f*(*n*) as functions of current at (a) 280 K and (b) 340 K. Insets: linear type. Calculated fractions of recombination mechanisms at (c) 10 mA and (d) 350 mA.

radiative efficiency, experiences a decrease upon temperature at both 10 mA [Fig. 4(c)] and 350 mA [Fig. 4(d)], This result is mainly due to the improvement of non-radiative processes at high-current and high-temperature levels, especially for the Auger recombination and carrier leakage, as clearly shown in insets of Figs. 4(a) and 4(b). Both contributions of Cn^3 and Dn^4 are intensified, but they exhibit a remarkably inverse temperature dependence at high current levels [Fig. 4(d)]. This drastic increase of Dn^4 indicates enhancement of carrier leakage, which is caused by high-energy electrons escape from being captured by MQWs, and most of electrons overflow outside the active layer due to the weak confinement of potentials at the well/barrier interfaces. Since Auger recombination is also related to the high-density and high-energy particles, the interplay among multiple carriers accelerates the energetic ones spill-out of MQWs. Therefore, as the temperature rises, the increase of coefficient *C* is attributed to the aggravated interaction of Auger-type particles promoted by the high temperature, while the decrease in the fraction of Cn^3 is due to the occurrence of Auger-induced leakage process. Besides, the severe defect-assisted emission, manifesting as the elevation of *An* term under high-current and high-temperature conditions, also results in electrons tunneling from MQWs along structure defects such as dislocations, further facilitating the carrier leakage from MQWs [31]. Consequently, both the Auger-induced process and the defect-assisted tunneling contribute to the carrier leakage, enhancing the non-radiative recombination and efficiency droop, particularly under the high forward current and the elevated temperatures. Meanwhile, the contribution of carrier leakage degrades the thermal stability and diminishes *m*, resulting in the decline of T_c and EQE with the forward current increases.

4. Conclusions

We analyze the temperature-dependent carrier recombination mechanisms of AlGaN-based DUV LEDs. Crystal defects stem from the mismatch in the MQWs, leading to the grievous SRH non-radiative recombination and low EQE. Both SRH term and carrier leakage strongly influence the thermal stability of EL. We suggest that Auger recombination and carrier leakage are mainly emphasized in the high injection case by the *m*-power method. Besides, we estimate individual recombination rates for SRH recombination, radiative recombination, Auger recombination, and carrier leakage by the $ABC + f(n)$ model. As the temperature rises, SRH recombination maintains a large proportion of the total recombination rate at lower forward currents. The enhanced Auger recombination and carrier leakage significantly affect the EQE droop when LEDs are subjected to high currents and high temperatures. Furthermore, the high-energy Auger recombination process assists the thermionic carrier leakage, which mainly includes carrier overflow from MQWs and defect-related tunneling process. In AlGaN-based DUV LEDs, the carrier leakage acts as a more important source for efficiency droop than in InGaN visible LEDs.

References

[1] M. Kneissl, T. Y. Seong, J. Han, and H. Amano, "The emergence and prospects of deep-ultraviolet light-emitting diode technologies," *Nature Photon.*, vol. 13, no. 4, pp. 233–244, 2019.

[2] J. G. Zhao *et al.*, "High internal quantum efficiency of nonpolar *a*-plane AlGaN-based multiple quantum wells grown on *r*-plane sapphire substrate," *ACS Photon.*, vol. 5, no. 5, pp. 1903–1906, 2018.

[3] N. Susilo *et al.*, "AlGaN-based deep UV LEDs grown on sputtered and high temperature annealed AlN/sapphire," *Appl. Phys. Lett.*, vol. 112, no. 4, 2018, Art. no. 041110.

[4] P. Du and Z. Cheng, "Enhancing light extraction efficiency of vertical emission of AlGaN nanowire light emitting diodes with photonic crystal," *IEEE Photon. J.*, vol. 11, no. 3, pp. 1–9, Jun. 2019.

[5] H. Yu *et al.*, "Enhanced performance of an AlGaN-based deep-ultraviolet LED having graded quantum well structure," *IEEE Photon. J.*, vol. 11, no. 4, pp. 1–6, Aug. 2019.

[6] X. Liu, K. Mashooq, T. Szkopek, and Z. Mi, "Improving the efficiency of transverse magnetic polarized emission from AlGaN based LEDs by using nanowire photonic crystal," *IEEE Photon. J.*, vol. 10, no. 4, pp. 1–11, Aug. 2018.

[7] Y. K. Ooi and J. Zhang, "Light extraction efficiency analysis of flip-chip ultraviolet light-emitting diodes with patterned sapphire substrate," *IEEE Photon. J.*, vol. 10, no. 4, pp. 1–13, Aug. 2018.

[8] Y. Zhao, H. Fu, G. T. Wang, and S. Nakamura, "Toward ultimate efficiency: Progress and prospects on planar and 3D nanostructured nonpolar and semipolar InGaN light-emitting diodes," *Adv. Opt. Photon.*, vol. 10, no. 1, pp. 246–308, 2018.

[9] J. Cho, E. F. Schubert, and J. K. Kim, "Efficiency droop in light-emitting diodes: Challenges and countermeasures," *Laser Photon. Rev.*, vol. 7, no. 3, pp. 408–421, 2013.

[10] X. Hai, R. T. Rashid, S. M. Sadaf, Z. Mi, and S. Zhao, "Effect of low hole mobility on the efficiency droop of AlGaN nanowire deep ultraviolet light emitting diodes," *Appl. Phys. Lett.*, vol. 114, no. 10, 2019, Art. no. 101104.

[11] A. Pandey, W. J. Shin, X. Liu, and Z. Mi, "Effect of electron blocking layer on the efficiency of AlGaN mid-ultraviolet light emitting diodes," *Opt. Exp.*, vol. 27, no. 12, pp. A738–A745, 2019.

[12] C. Liu, Y. K. Ooi, S. M. Islam, H. Xing, D. Jena, and J. Zhang, "234 nm and 246 nm AlN-Delta-GaN quantum well deep ultraviolet light-emitting diodes," *Appl. Phys. Lett.*, vol. 112, no. 1, 2018, Art. no. 011101.

[13] M. Auf der Maur, A. Pecchia, G. Penazzi, W. Rodrigues, and A. Di Carlo, "Efficiency drop in green InGaN/GaN light emitting diodes: The role of random alloy fluctuations," *Phys. Rev. Lett.*, vol. 116, no. 2, 2016, Art. no. 027401.

[14] E. A. Clinton, Z. Engel, E. Vadiee, J. V. Carpenter, Z. C. Holman, and W. A. Doolittle, "Ultra-wide-bandgap AlGaN homojunction tunnel diodes with negative differential resistance," *Appl. Phys. Lett.*, vol. 115, no. 8, 2019, Art. no. 082104.

[15] T. Z. Wu *et al.*, "Interplay of carriers and deep-level recombination centers of 275-nm light-emitting diodes—Analysis on the parasitic peaks over wide ranges of temperature and injection density," *Opt. Exp.*, vol. 27, no. 16, pp. A1060–A1073, 2019.

[16] T. J. Yang, R. Shivaraman, J. S. Speck, and Y. R. Wu, "The influence of random indium alloy fluctuations in indium gallium nitride quantum wells on the device behavior," *J. Appl. Phys.*, vol. 116, no. 11, 2014, Art. no. 113104.

[17] Q. Dai *et al.*, "Carrier recombination mechanisms and efficiency droop in GaInN/GaN light-emitting diodes," *Appl. Phys. Lett.*, vol. 97, no. 13, 2010, Art. no. 133507.

[18] N. Trivellin *et al.*, "Degradation processes of 280 nm high power DUV LEDs: Impact on parasitic luminescence," *Jpn. J. Appl. Phys.*, vol. 58, no. SC, 2019, Art. no. SCCC19.

[19] L. Zhao *et al.*, "Temperature-dependent efficiency droop in GaN-based blue LEDs," *IEEE Electron Device Lett.*, vol. 39, no. 4, pp. 528–531, Apr. 2018.

[20] C. C. Pan *et al.*, "Reduction in thermal droop using thick single-quantum-well structure in semipolar (2021) blue light-emitting diodes," *Appl. Phys. Exp.*, vol. 5, no. 10, 2012, Art. no. 102103.

[21] X. A. Cao, S. F. LeBoeuf, and T. E. Stecher, "Temperature-dependent electroluminescence of AlGaN-based UV LEDs," *IEEE Electron Device Lett.*, vol. 27, no. 5, pp. 329–331, May 2006.

[22] X. Feng, K. Wang, Y. Cheng, Y. Wei, and T. Yu, "High-performance near-UV LED grown by carbon nanotube assisted nanoheteroepitaxy," *Superlattices Microstructures*, vol. 109, pp. 41–46, 2017.

[23] K. S. Kim, D. P. Han, H. S. Kim, and J. I. Shim, "Analysis of dominant carrier recombination mechanisms depending on injection current in InGaN green light emitting diodes," *Appl. Phys. Lett.*, vol. 104, no. 9, 2014, Art. no. 091110.
[24] Y. J. Lee *et al.*, "Study of the excitation power dependent internal quantum efficiency in InGaN/GaN LEDs grown on patterned sapphire substrate," *IEEE J. Sel. Topics Quantum Electron.*, vol. 15, no. 4, pp. 1137–1143, Jul./Aug. 2009.
[25] G. B. Lin, D. Meyaard, J. Cho, E. F. Schubert, H. Shim, and C. Sone, "Analytic model for the efficiency droop in semiconductors with asymmetric carrier-transport properties based on drift-induced reduction of injection efficiency," *Appl. Phys. Lett.*, vol. 100, no. 16, 2012, Art. no. 161106.
[26] Y. Sun *et al.*, "Optical excitation study on the efficiency droop behaviors of InGaN/GaN multiple-quantum-well structures," *Appl. Phys. B*, vol. 114, no. 4, pp. 551–555, 2014.
[27] Q. Dai *et al.*, "On the symmetry of efficiency-versus-carrier-concentration curves in GaInN/GaN light-emitting diodes and relation to droop-causing mechanisms," *Appl. Phys. Lett.*, vol. 98, no. 3, 2011, Art. no. 033506.
[28] G. D. Hao, N. Tamari, T. Obata, T. Kinoshita, and S. I. Inoue, "Electrical determination of current injection and internal quantum efficiencies in AlGaN-based deep-ultraviolet light-emitting diodes," *Opt. Exp.*, vol. 25, no. 16, pp. A639–A648, 2017.
[29] H. Y. Ryu, I. G. Choi, H. S. Choi, and J. I. Shim, "Investigation of light extraction efficiency in AlGaN deep-ultraviolet light-emitting diodes," *Appl. Phys. Exp.*, vol. 6, no. 6, 2013, Art. no. 062101.
[30] J. Yun, J. I. Shim, and H. Hirayama, "Analysis of efficiency droop in 280-nm AlGaN multiple-quantum-well light-emitting diodes based on carrier rate equation," *Appl. Phys. Exp.*, vol. 8, no. 2, 2015, Art. no. 022104.
[31] L. V. Asryan, "Effect of pumping delay on the modulation bandwidth in double tunneling-injection quantum dot lasers," *Opt. Lett.*, vol. 42, no. 1, pp. 97–100, 2017.